A Cavopulmonary Assist Device for long-term Therapy of Fontan Patients

Andreas Escher MSc , Carsten Strauch MSc , Emanuel J. Hubmann MSc , Prof. Michael Hübler MD , Dominik Bortis PhD , Bente Thamsen PhD , Marc Mueller PhD , Ulrich Kertzscher PhD , Prof. Paul U. Thamsen PhD , Prof. Johann W. Kolar PhD , Prof. Daniel Zimpfer MD , Marcus Granegger PhD

PII: S1043-0679(21)00297-5
DOI: https://doi.org/10.1053/j.semtcvs.2021.06.016
Reference: YSTCS 1984

To appear in: *Seminars in Thoracic and Cardiovascular Surgery*

Please cite this article as: Andreas Escher MSc , Carsten Strauch MSc , Emanuel J. Hubmann MSc , Prof. Michael Hübler MD , Dominik Bortis PhD , Bente Thamsen PhD , Marc Mueller PhD , Ulrich Kertzscher PhD , Prof. Paul U. Thamsen PhD , Prof. Johann W. Kolar PhD , Prof. Daniel Zimpfer MD , Marcus Granegger PhD , A Cavopulmonary Assist Device for long-term Therapy of Fontan Patients, *Seminars in Thoracic and Cardiovascular Surgery* (2021), doi: https://doi.org/10.1053/j.semtcvs.2021.06.016

A Cavopulmonary Assist Device for long-term Therapy of Fontan Patients

Andreas Escher, MSc[1,2], Carsten Strauch, MSc[3], Emanuel J. Hubmann, MSc[4], Prof. Michael Hübler, MD[5], Dominik Bortis, PhD[4], Bente Thamsen, PhD[1], Marc Mueller, PhD[6], Ulrich Kertzscher, PhD[1], Prof. Paul U. Thamsen, PhD[3], Prof. Johann W. Kolar, PhD[4], Prof. Daniel Zimpfer, MD[2], Marcus Granegger, PhD[1,2]

[1] Biofluid Mechanics Laboratory, Institute for Imaging Science and Computational Modelling in Cardiovascular Medicine, Charité-Universitätsmedizin Berlin, Berlin, Germany

[2] Department of Cardiac Surgery, Medical University of Vienna, Vienna, Austria

[3] Fachgebiet für Fluidsystemdynamik, Technische Universität Berlin, Berlin, Germany

[4] Power Electronic Systems Laboratory, ETH Zurich, Zurich, Switzerland

[5] University Heart & Vascular Center, University Medical Center Hamburg-Eppendorf, Hamburg, Germany

[6] Institute for Multiphase Processes, Leibniz University Hannover, Hannover, Germany

Conflict of Interest: Marcus Granegger received personal fees and grants from BerlinHeart GmbH; Ulrich Kertzscher received grants from Berlin Heart GmbH.

Sources of Funding*:* This study was supported by the GIGAX Foundation.

Corresponding author:

Marcus Granegger, PhD

Department of Cardiac Surgery

Medical University of Vienna

AKH Wien, Währinger Gürtel 18-20

A-1090 Wien

Phone: +43 1 4040055390

Fax: +43 1 4040067890

Email: marcus.granegger@meduniwien.ac.at

Central Picture

Preclinical proof of a novel assist device for chronic support in Fontan patients.

Central Message

A novel cavopulmonary assist device showed little traumatic potential at low power consumption and across a comprehensive clinically relevant range of hemodynamic conditions in Fontan patients.

Perspective Statement

Long-term cavopulmonary support remains in its infancy. This study presents a novel cavopulmonary assist device for chronic support in an inclusive Fontan patient population. *In-silico* and *in-vitro* analysis delivered the preclinical proof for a fully implantable, hemocompatible device design. Acute and chronic *in-vivo* trials are proposed to support laboratory findings.

Structured Abstract

Objective: Treatment of univentricular hearts remains restricted to palliative surgical corrections (Fontan pathway). The established Fontan circulation lacks a sub-pulmonary pressure source and is commonly accompanied by progressively declining hemodynamics. A novel cavopulmonary assist device (CPAD) may hold the potential for improved therapeutic management of Fontan patients by chronic restoration of biventricular equivalency. This study aimed at translating clinical objectives towards a functional CPAD with preclinical proof regarding hydraulic performance, hemocompatibility and electric power consumption.

Methods: A prototype composed of hemocompatible titanium components, ceramic bearings, electric motors, and corresponding drive unit was manufactured for preclinical benchtop analysis: hydraulic performance in general and hemocompatibility characteristics in particular were analyzed *in-silico* (computational fluid dynamics) and validated *in-vitro*. The CPAD's power consumption was recorded across the entire operational range.

Results: The CPAD delivered pressure step-ups across a comprehensive operational range (0-10L/min, 0-50mmHg) with electric power consumption below 1.5W within the main operating range. *In-vitro* hemolysis experiments (N=3) indicated a normalized index of hemolysis (NIH) of 3.8±1.6mg/100L during design point operation (2500rpm, 4L/min).

Conclusions: Preclinical investigations revealed the CPAD's potential for low traumatic and thrombogenic support of a heterogenous Fontan population (pediatric and adult) with potentially accompanying secondary disorders (e.g. elevated pulmonary vascular resistance or systemic ventricular insufficiency) at distinct physical activities. The low power consumption implied adequate settings for a small, fully implantable system with transcutaneous energy transfer. The successful preclinical proof provides the rationale for acute and chronic *in-vivo* trials aiming at the confirmation of laboratory findings and verification of hemodynamic benefit.

Keywords:

Fontan, chronic cavopulmonary assist device, mechanical circulatory support, rotary blood pump

Glossary of Abbreviations

UVH – univentricular heart

TCPC – total cavopulmonary connection

MCS – mechanical circulatory support

PVR – pulmonary vascular resistance

CPAD – cavopulmonary assist device

IVC – inferior vena cave

SVC – superior vena cave

LPA – left pulmonary artery

RPA – right pulmonary artery

PVDF-TrFE – polyvinylidene fluoride-co-trifluoroethylene

SV – single ventricle

CAD – computer aided design

IR – inflow ratio

TET – transcutaneous energy transfer

CFD – computational fluid dynamics

NIH – normalized index of hemolysis

IU – international unit

fHb – plasma-free hemoglobin

SD – standard deviation

RBP – rotary blood pump

HM3 – HeartMate 3

HVAD – HeartWare Ventricular Assist Device

LVAD – left ventricular assist device

HLRN – North-German Supercomputing Alliance

VSC – Vienna Scientific Cluster

Graphical Abstract

Preclinical proof of a novel assist device for chronic support in Fontan patients

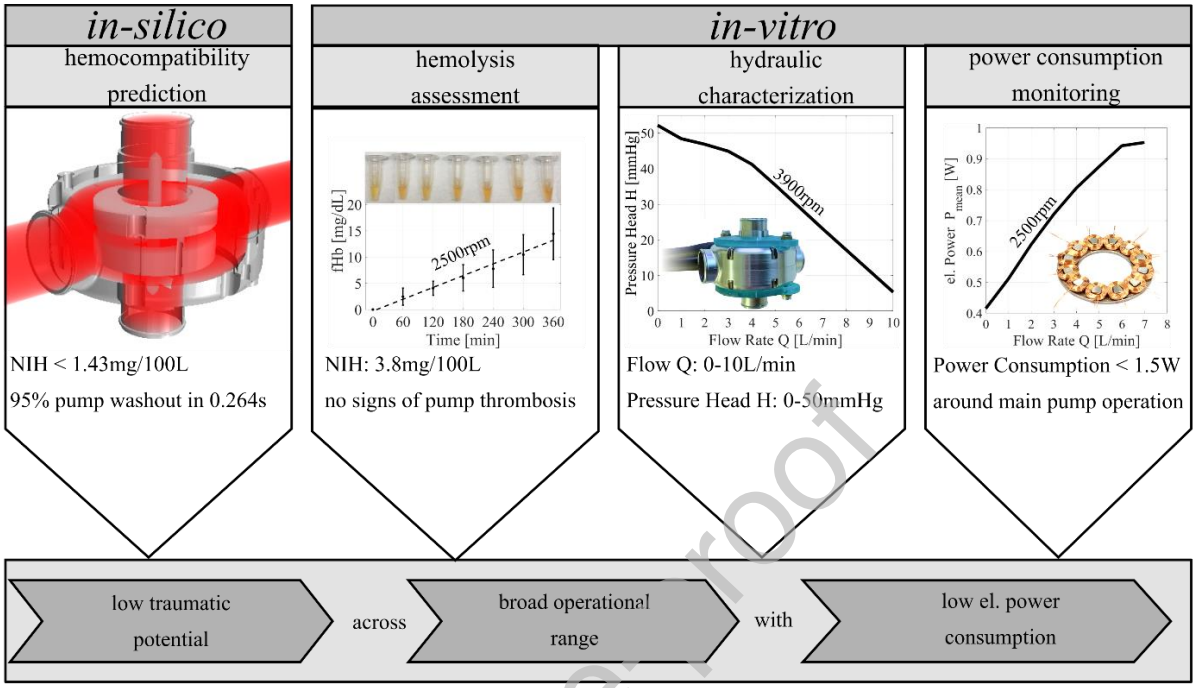

NIH: normalized index of hemolysis; Q: flow rate; H: pressure head

Preclinical evaluation (in-silico, in-vitro) of the CPAD indicated the potential for low traumatic support at low power consumption and across a broad range of hemodynamic conditions (Q=0-10L/min, H=0-50mmHg). CPAD: cavopulmonary assist device; Q: flow rate; H: pressure head.

Introduction

Univentricular hearts (UVHs) account for approximately 10% of all congenital heart defects.[1] The majority of patients with UVH undergo a Fontan type palliation with total cavopulmonary connection (TCPC).[2] Given the absence of a sub-pulmonary ventricle after TCPC completion, pulmonary perfusion is driven by elevated central venous pressures. This is associated with several long-term complications directly related to chronic venous congestion including lymphatic dysfunction, reduced cardiac output and liver fibrosis.[3–5] These complications ultimately result in a failing Fontan circulation[6,7] that presents a primary source of mortality in patients with UVH.

Currently, cardiac transplantation is the only long-term treatment option for patients with failing Fontan circulation. However, due to the limited availability of donor hearts and the complexity of the procedure,[8] cardiac transplantation remains controversially discussed. Meanwhile, the living Fontan population is predicted to double within the next 20 years,[9] underpinning the medical need for alternative long-term treatment strategies.

Mechanical circulatory support (MCS) in failing Fontan patients is challenging and has only been anecdotally reported,[10–19] with poorer results than in biventricular patients with heart failure.[15]

Recent advances in the field led to the introduction of MCS devices that are specifically intended for chronic cavopulmonary support.[20,21] Despite the seminal potential of those concepts, it remains unclear whether they meet the clinical demands to adequately support the heterogeneous Fontan population ranging from pediatric to adult patients with individual pursuits of physical activity and potentially accompanying secondary disorders (e.g. elevated pulmonary vascular resistance (PVR) or systemic ventricular insufficiency).

Within an interdisciplinary initiative to meet the medical need for a durable MCS option accessible to an inclusive Fontan population we recently introduced a cavopulmonary assist device (CPAD) specifically designed to substitute the missing sub-pulmonary ventricle.[22] The aim of the present study was to translate clinical objectives into a corresponding functional, hemocompatible CPAD with subsequent preclinical evaluation. Focus was laid on clinically relevant aspects including the interaction between the CPAD and the cardiovascular system, hemocompatibility as well as electric power consumption.

Material and Methods

CPAD – Clinical Requirements and Device Design

Mechanical Design and Vascular Connection

Clinical requirements regarding the anatomical compliance of a CPAD include the demand for (i) small-sized conception to prevent squeezing of surrounding sensible structures, (ii) high durability for chronic application as well as (iii) versatile and stable vascular connection to fit an inclusive range of patients.

Above requirements were translated into the CPAD design (Figure 1D). Once implanted (Figure 1A), blood from the inferior (IVC) and superior vena cava (SVC) is entering the flow chamber (Figure 1B-C) via two inflow cannulae (Ø11mm), while being rerouted into the left (LPA) and right pulmonary artery (RPA), respectively, along two outflow cannulae (Ø12mm). Distal ends of the cannula in- and outlets are spaced by 34mm and 40mm, respectively.

Pressure rise is generated by a four-bladed impeller (Ø19mm, h=9.5mm, medical-grade titanium). The impeller is supported within a circular flow chamber (Ø30mm, h=19mm, medical grade titanium) using blood-immersed mechanical ball-cup bearings (ball: ruby, cup: silicon-carbide whiskers reinforced aluminum oxide) (Figure 1B).

Versatile anastomosis of the CPAD to the patient-specific vasculature is realized with custom-made conical grafts. Designed for a diameter evolving from 20 to 11mm on the inflow (IVC, SVC), and from 12 to 20mm on the outflow side (LPA, RPA), respectively (Figure 1C, bottom), the grafts are to be surgically secured on the respective in- and outflow cannulae. The conical shape permits graft shortening to the required vessel diameter facilitating optimal vascular anastomosis. The grafts were manufactured with a previously developed electrospinning device[23] (conically shaped rotating collector: 1000rpm, flow rate: 3.5ml/h, applied voltage: 20kV, needle diameter: 0.8mm, spinning time: 15min). Polyvinylidene fluoride-co-trifluoroethylene (PVDF-TrFE) with a concentration of 20wt% dissolved in N,N-dimethylformamide and acetone (6:4) was used for graft fabrication.

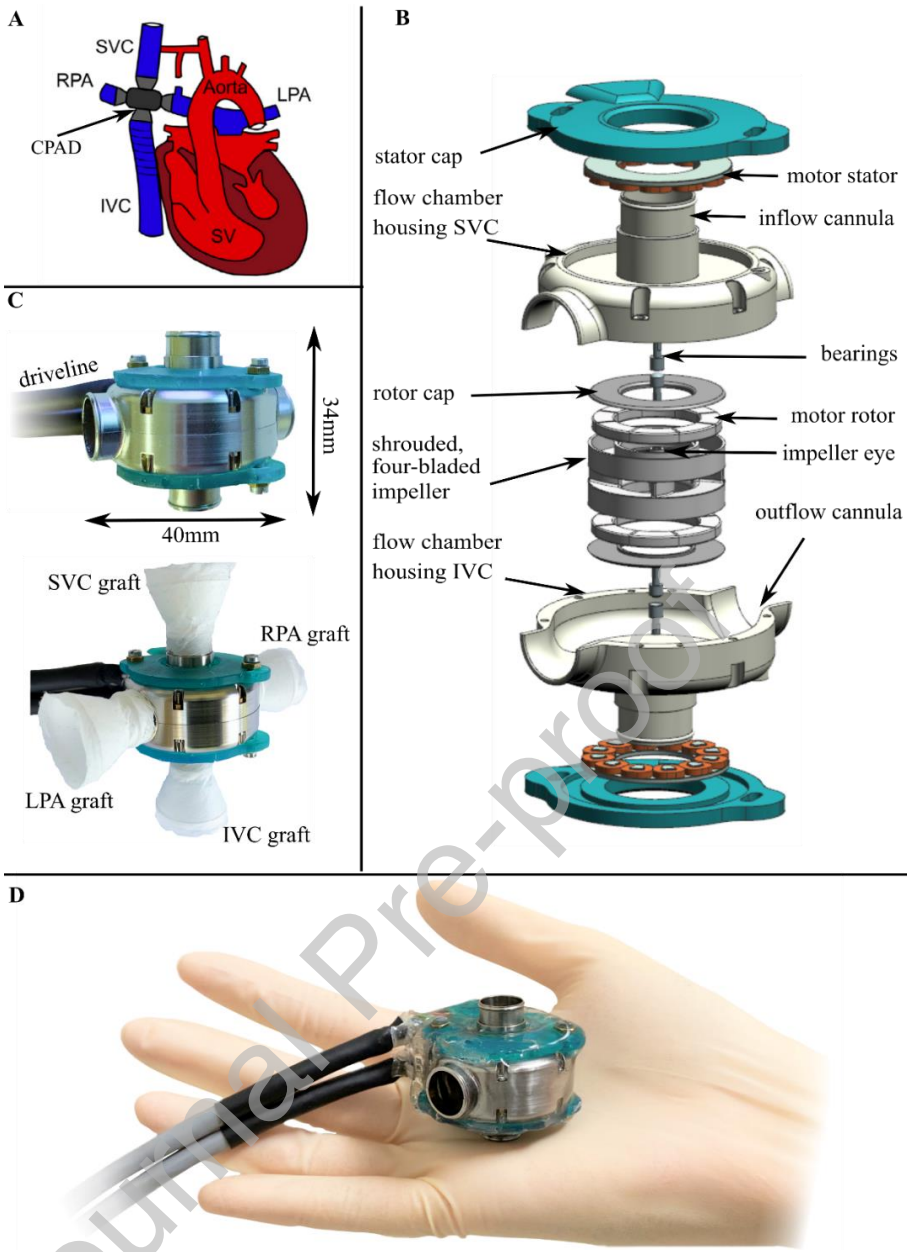

Figure 1. Mechanical design of the CPAD for implantation in TCPC position. A. CPAD implanted in TCPC location between IVC, SVC, LPA and RPA in a heart with single ventricle.[22] Blood is entering the flow chamber through its inflow cannulae that are connected to the IVC and SVC, and radially ejected through its outlet cannulae which are anastomosed to the LPA and RPA, respectively. B. CAD explosion view of the CPAD that is composed of a four-bladed impeller which is suspended within the circular flow chamber using mechanical ball-cup bearings. Via driveline, the impeller is actuated by the electromagnetic force that is generated by the coupling between motor rotor and motor stator. The stators are protected from corrosion by means of 3D-printed stator cap prototypes. C. Functional prototype of the CPAD (top) including the setting with both its in- and outlets connected to the custom-made electrospun conical grafts (bottom). Distal ends of the cannula in- and outlets are spaced by 34mm and 40mm, respectively. The total volume of the CPAD amounts to a magnitude of 17.8cm^3. D. Illumination of the small-sized conception of the current functional prototype. CPAD: cavopulmonary assist device; TCPC: total cavopulmonary connection; IVC: inferior vena cava; SVC: superior vena cava; LPA: left pulmonary artery: RPA: right pulmonary artery; SV: single ventricle; CAD: computer aided design.

Hydraulic Design

The support of a heterogenous Fontan population with potentially accompanying secondary disorders (e.g. elevated PVR or systemic ventricular insufficiency) at distinct physical activities may require diversified magnitudes of flow and cavopulmonary pressure rises. Accordingly, clinical requirements for a CPAD include the demand for (i) efficient operation across a broad range of flow (Q=0-10L/min) and pressure heads (H=0-50mmHg) to provide freedom for physiologically-controlled support of pediatric and adult patients across all clinically relevant conditions, (ii) to increase blood flow with rising venous return, (iii) to exhibit low resistance towards venous return in the event of stalled pump condition, (iv) to operate at low traumatic and thrombogenic potential and (v) to deliver a homogenous mixture of the hepatic factor to the left and right lung. Loss of the hepatic factor may lead to the degeneration of the pulmonary vasculature.[24]

Above demands were accounted for in the hydraulic conception of the CPAD. Based on turbomachinery principles the CPAD was hydraulically designed for a rotational speed (n) of 2500rpm and flow rates of 4L/min (design point). An imbalanced inflow ratio (IR) of Q_{IVC}/Q_{SVC}=2:1 was deemed representative for a typical condition in young adolescent Fontan patients.[25] Gap dimensions (w=500μm) were designed as a trade-off accounting for efficient operation, appropriate motor cooling, prevention of pump occlusion (passage of floating thrombi) and reduction of flow obstruction during dysfunctional condition.

Actuation Design

Clinical requirements for the electric actuation of a CPAD include the demand for (i) efficient operation to prevent local blood temperature rises above 2°C due to motor heat losses (ISO14708-1), (ii) low power consumption to enable the integration of transcutaneous energy transfer (TET) technologies, (iii) a failsafe design to prevent device dysfunction, and (iv) minimal dimensions to fit within the small-sized CPAD.

An electric motor complying with above requirements was previously optimized for its specific application in this CPAD.[26] To ensure a failsafe design, the motor concept was realized by a redundant axial-flux three-phase synchronous motor configuration with stators in the upper and lower flow chamber casing, respectively, and permanent magnets integrated at the top and bottom of the impeller (Figure 1B). Motor stators were sealed with epoxide resin, each of which covered with a 3D-printed stator cap prototype (Formlabs, Massachusetts, USA) (Supplementary Section 1).

Evaluation of Hydraulic Characteristics, Hemocompatibility and Power Consumption

In-silico Hemocompatibility Prediction

Compliance of the CPAD with stipulated clinical demands regarding hydraulic performance was verified using computational fluid dynamics (CFD) with the package Star CCM+ (Siemens, Munich, Germany) (Figure 2A, Supplementary Section 2).

As a measure of hemocompatibility, normalized indices of hemolysis (NIH) were computed[27] and volume portions exposed to shear stresses above 9, 50 and 150Pa, respectively, identified.[28,29] The corresponding analysis was performed for an IR of 2:1 across the operational range.

In addition, a passive scalar transport model was incorporated for virtual pump washout analysis during design point operation. The same routine was followed to evaluate the distribution of the hepatic factor to both the LPA and RPA, respectively, for IR's of 2:1 and 3:1. Blood stagnation was defined for velocities below 0.1m/s,[28,29] thus complementing the washout analysis to predict the thrombotic potential within the pump.

In-vitro Hydraulic Characterization and CFD Validation

For *in-vitro* validation of CFD data, a hydraulic testbench was recently realized,[30] specifically tailored to accurately characterize hydraulic performance of the CPAD (Supplementary Section 3). Via 3/8'' silicon tubings the CPAD was integrated into the four TCPC-mimicking flow paths of the *in-vitro* testbench (Figure 2B). The testbench was filled with blood analogue (water-glycerol mixture, ρ=1110kg/m^3, μ=3.0mPa s, T=37°C) while pressure heads and flow rates were recorded for pump operation at rotational speeds of n=1500-3900rpm for both balanced (Q_{IVC}/Q_{SVC}=1:1) and imbalanced (Q_{IVC}/Q_{SVC} =2:1, Q_{IVC}/Q_{SVC} =3:1) IR's.

Potential flow obstruction imposed by a failing CPAD was furthermore inspected by recording the pressure drop across the pump during stalled pump condition (n=0rpm).

In-vitro Hemolysis Assessment

Hemolysis experiments were conducted as previously described,[28] in accordance with ASTM-F1841-97 standards, and with the prototype actuated at design point operation. In each experiment, 600mL of heparinized bovine blood (15'000 international units (IU) per 5L) was circulating within the circuit. Sample extraction (2mL) was performed every 60 minutes.

Upon twofold sample centrifugation at 5600xg during 15min for plasma isolation (Microfuge 22R Centrifuge, Beckman Coulter, California, USA) and subsequent dilution of 100µL of the plasma with 1000µL of sodium carbonate, plasma-free hemoglobin (fHb) was photometrically determined (Photometer 4040_V5+ Robert Riele GmbH & Co KG, Berlin, Germany).

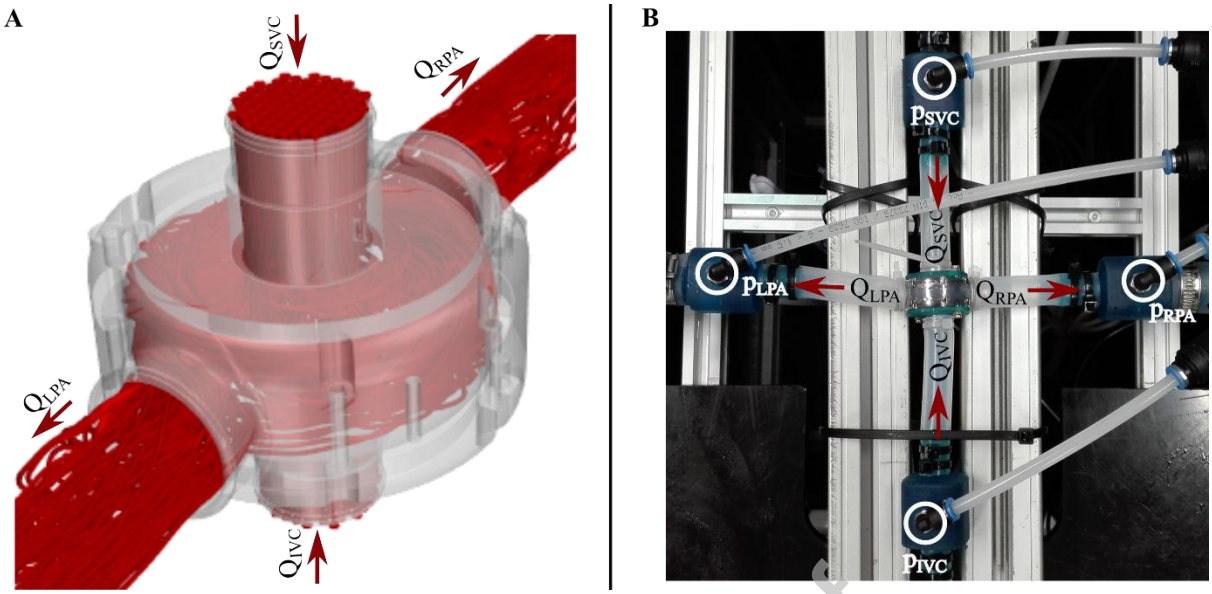

Figure 2. In-silico and in-vitro hydraulic characterization of the CPAD. A. In-silico setup for hydraulic characterization and hemolysis prediction numerically showing the blood circulation through the CPAD. B. CPAD connected to the TCPC-imitating configuration of the in-vitro testbench. The functional prototype of the CPAD was integrated into the testbench via four 3/8'' silicon tubings of equal length (L=65mm) that were furthermore connected to the four pressure sensors (p_{IVC}, p_{SVC}, p_{LPA}, p_{RPA}). White circles denote the pressure sensors, while the red arrows indicate blood flow direction. CPAD: cavopulmonary assist device; TCPC: total cavopulmonary connection; p_{SVC}: pressure superior vena cava; p_{IVC}: pressure inferior vena cava; p_{LPA}: pressure left pulmonary artery; p_{RPA}: pressure right pulmonary artery.

Monitoring of Electric Power Consumption

Compliance with the clinical demand for low electric power consumption was verified by the acquisition of motor input phase-voltage and phase-current (current transducer LA 25-NP/SP9, LEM Europe GmbH, Hessen, Germany). Signals were sampled at 20kHz across the operational range using a dSPACE MicroLAB Box (dSPACE GmBH, Paderborn, Germany). Mean electric power consumption of the CPAD was computed over periods of 50s:

Electric Power Consumption [W]: $$P_{el,mean} = \sum_{ph=1}^{3} \left(\frac{1}{N_t} \sum_{t_0}^{t_{end}} u_{ph}(t) \cdot i_{ph}(t) \right) \quad \text{(Eq. 1)}$$

where ph denotes the phase [-], u_{ph} the phase-voltage [V], i_{ph} the phase-current [A], N_t the number of time steps [-], t the time [s], t_0 the start and t_{end} the end time of power recording [s], respectively.

Results

Hydraulic and Hemocompatibility Characteristics

In-silico Hemocompatibility Properties

CFD data showed the CPAD to operate at hydraulic efficiencies (η_{hyd}) (Supplementary Section 4) above 30% across a broad range (Q=2-8L/min). Peak efficiencies were identified around design point operation (η_{hyd}=45.79%) (Figure 3A).

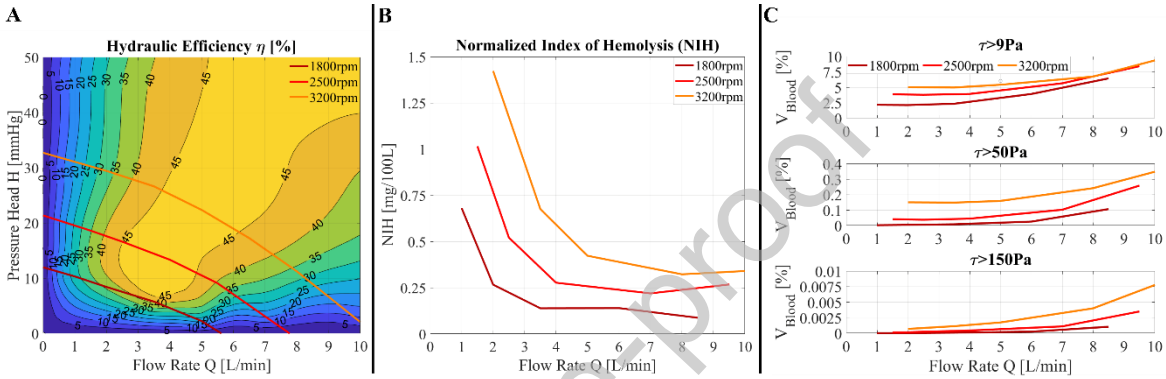

Figure 3. In-silico hydraulic performance and blood trauma prediction. A. Numerically computed hydraulic efficiency of the CPAD with three exemplary pressure-flow curves (n=1800, 2500, 3200rpm, IR=2:1) indicating a comprehensive operational range of high hydraulic efficiency (η_{hyd}>30%) performance. B. Numerically predicted NIH for the CPAD operated at rotational speeds of 1800, 2500 and 3200rpm with an IR of 2:1 indicating an increase towards low-flow operation, however with low-level values (NIH<1.43mg/100L) across a broad clinically relevant range. C. Computed blood volume portions exposed to shear stresses above 9, 50 and 150Pa across the pump's operational range (IR=2:1), expressed as percentage of the pump's priming volume. Volumes exposed to the respective shear stress levels tend to increase with increasing flow rate. CPAD: cavopulmonary assist device; n: rotational speed; IR: inflow ratio; NIH: normalized index of hemolysis.

The numerically predicted NIH increased during low-flow, low-efficiency operation (Q=1-3L/min, Figure 3B). However, peak values remained below 1.43mg/100L across the clinically relevant range. Blood volumes exposed to shear stresses above 9, 50 and 150Pa remained below 10, 0.4 and 0.01% of the priming volume in the CPAD, respectively, with noticeable rise towards increasing flow rates (Figure 3C).

At design point operation, 90 and 95% of the old blood was washed out within t_{90}=0.21s (8.7 revolutions) and t_{95}=0.26s (11 revolutions), respectively (Figure 4A). Further, blood stagnation with velocities below 0.1m/s was observed in 1.77% of the entire priming volume.

In the event of imbalanced IR's, the CPAD delivered well-mixed homogeneous outflow to both LPA (50.2% and 49.6% of IVC blood during 2:1 and 3:1 IR condition, respectively) and RPA (49.8% and 50.4% of IVC blood during 2:1 and 3:1 IR condition, respectively) (Figure 4B).

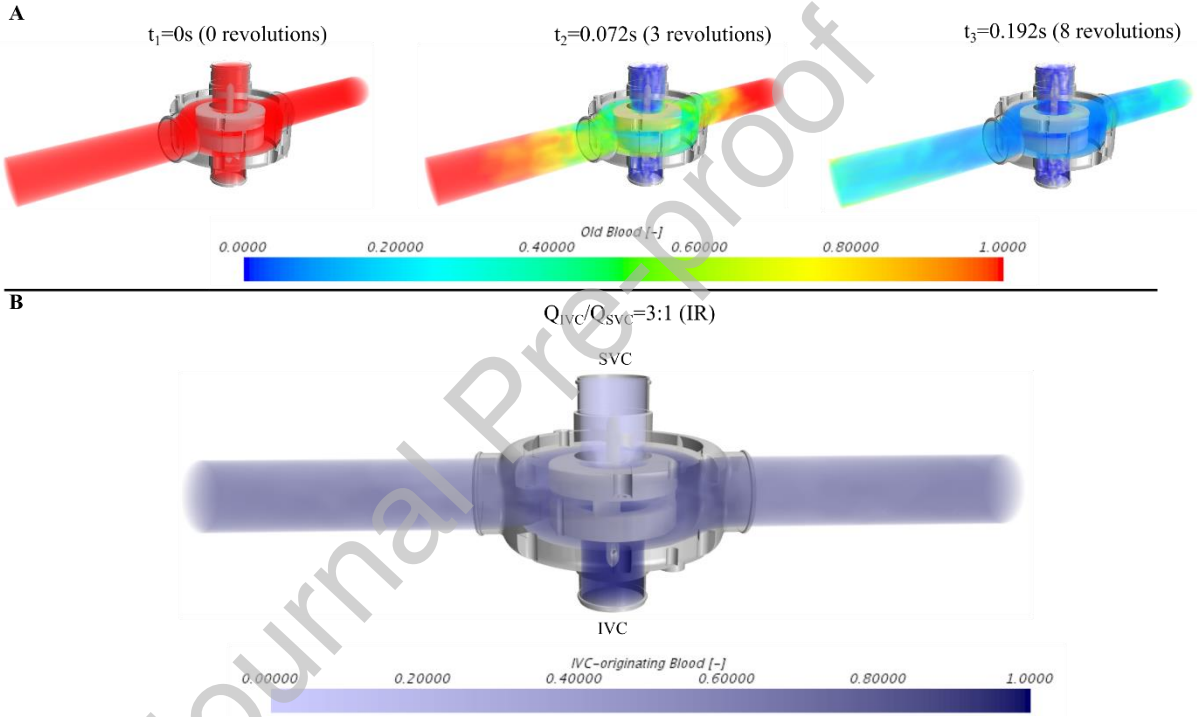

Figure 4. Numerical prediction of old blood washout and IVC/SVC blood mixing behavior. A. In the process of the virtual washout experiment the CPAD is run with design point settings (n=2500rpm, Q=4L/min, H=12.55mmHg, IR=2:1), while old blood (visualized in red, t_1) is continuously replaced with the newly entering blood represented in blue. After 3 revolutions (t_2=0.072s) the new blood is increasingly mixing with the old blood consequently displacing the old blood towards the LPA and RPA outlets. After 8 revolutions (t_3=0.192s), 87.83% of the old blood is replaced with new blood. B. During design point operation (n=2500rpm, Q=4L/min, H=12.55mmHg), however, with highly imbalanced IR of 3:1 blood that is entering through the IVC (denoted as dark blue) is homogeneously mixed with the inflowing blood of the SVC, equalizing outflow distribution of IVC-blood to both LPA and RPA outlet. IVC: inferior vena cava; SVC: superior vena cava; LPA: left pulmonary artery; RPA: right pulmonary artery; CPAD: cavopulmonary assist device; n: rotational speed; Q: flow rate; H: pressure head; IR: inflow ratio.

In-vitro Hydraulic Properties and CFD Validation

Figure 5 depicts the *in-vitro* pressure-flow relationship of the CPAD, illustrated as mean and standard deviation (SD) among different IR's (1:1, 2:1, 3:1). Error bars indicate marginal deviations in generated pressure heads among different IR's (SD<1.12mmHg).

The CPAD provided support across a broad range with maintained pressure step-up's at high flow rates (Q>10L for n>3200rpm) and peak pressure heads of 52.68mmHg (Q=0L/min, n=3900rpm).

Pressure losses across the CPAD (light green line, Figure 5) in case of pump failure (n=0rpm, pump stalled) ranged from 0.31 to 6.3mmHg with resistances between 0.63 to 3.15mmHg/(L/min) (Wood Units) for flow rates within 1 to 4L/min.

Hydraulic *in-vitro* measurements showed good agreement (H: RMSE<0.92mmHg) with pressure-flow characteristics calculated using CFD (black markers, Figure 5, Supplementary Section 5).

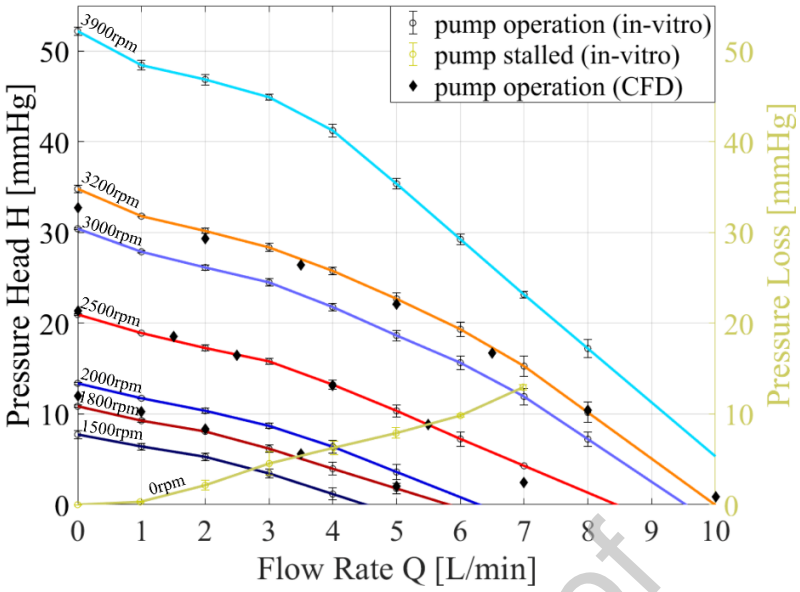

Figure 5. Pressure-flow relationship indicating the hydraulic performance of the CPAD. Pressure heads were recorded in-vitro for the operation at rotational speeds between 1500 and 3900rpm with flow rates ranging from 0 to 8L/min. At each flow rate, in-vitro data is presented as mean and standard deviation (error bars) among pressure heads recorded for balanced (1:1) and imbalanced (2:1, 3:1) IR's. Black makers represent the numerically computed pressure-flow relationship (CFD) at selected rotational speeds (1800, 2500, 3200rpm) for flow rates among 0 to 10L/min and an IR of 2:1. Pressure-loss across the CPAD in case of stalled pump condition (n=0rpm) is illustrated as light green line. CPAD: cavopulmonary assist device; IR: inflow ratio; CFD: computational fluid dynamics; n: rotational speed.

In-vitro Hemolysis

Blood was circulating within the *in-vitro* mock loop in three distinct experiments (N=3) of 6h each (Figure 6). The experimentally determined NIH revealed a value of 3.8±1.6mg/100L, while no signs of any depositions were observed throughout the experiments.

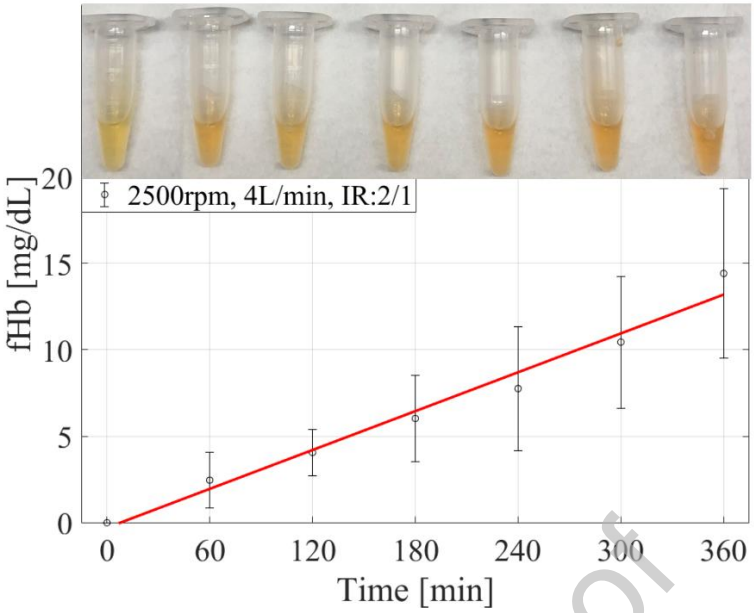

Figure 6. In-vitro hemolysis assessment. Increasing concentration of plasma free hemoglobin (fHb) during in-vitro hemolysis experiments (N=3) of 6h design point operation each (2500rpm, 4L/min, IR=2:1). At each sampling time point (Δt=60min), in-vitro data is presented as median and standard deviation (error bars) of the photometrically determined concentration in plasma free hemoglobin across the three distinct experiments. The top row shows the Eppendorf tubes with isolated blood plasma at each sampling time, illustrating the rise of plasma free hemoglobin by increasing red-scale over time. fHb: free Hemoglobin; N: number of experiments; IR: inflow ratio.

Electric Power Consumption

The electric power consumption of the CPAD increased with rotational speeds (Figure 7). It disclosed monotonic dependence on the flow rate with marginal sensitivity to variations in IR (SD<0.13W). During design point operation the CPAD run at 0.83W while the power consumption remained below 1.5W within the main operating range. Peak values of 3.24W were measured during off-design operation (n=3900rpm, Q=8L/min, H=18.22mmHg).

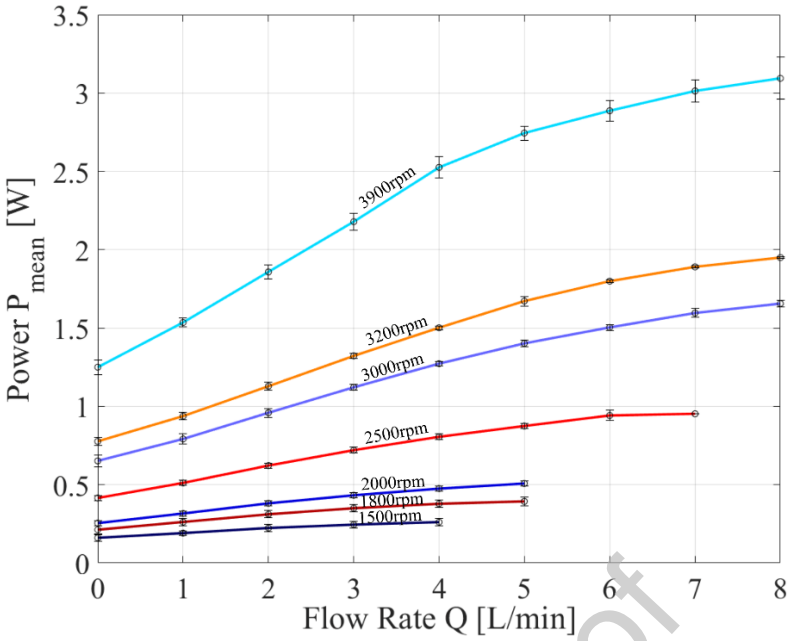

Figure 7. Electric power consumption of the CPAD. The power consumption was monitored across a clinically relevant range with flow rates between 0 to 8L/min and at rotational speeds of 1500 to 3900rpm, showing monotonic behavior across the entire operational range. Measured data is presented at each flow rate as mean and standard deviation (error bars) among balanced (1:1) and imbalanced (2:1, 3:1) IR's with the solid line representing the interpolation between measurement points. CPAD: cavopulmonary assist device; IR: inflow ratio.

Discussion

This study aimed at (i) the translation of key clinical demands for cavopulmonary support towards a functional prototype and (ii) the verification of its compliance with clinical demands regarding hydraulic performance, hemocompatibility and electric power consumption.

We delivered the proof-of-feasibility to manufacture the previously proposed novel CPAD[22] in an advanced prototype that meets key demands regarding hemocompatibility, robustness and vascular connection. Pump components complied with material selections of widespread application in implantable blood pumps with a bearing design that comes with long-term experience in both hemocompatibility and durability given its low wear profile.[31] Previous

results pointed towards low-level bearing forces combined with a well-washed bearing configuration, which may mitigate the risk of heat generation and thrombus deposition.[22]

Further, the electrospun grafts provide the potential for versatile, leak-tight and tear-resistant anastomosis of the CPAD to patient-specific vasculatures. *In-silico* and *in-vitro* findings revealed the CPAD to operate at low traumatic and thrombogenic potential with little electric power consumption across a comprehensive range of clinically relevant hemodynamic conditions (Figure 8).

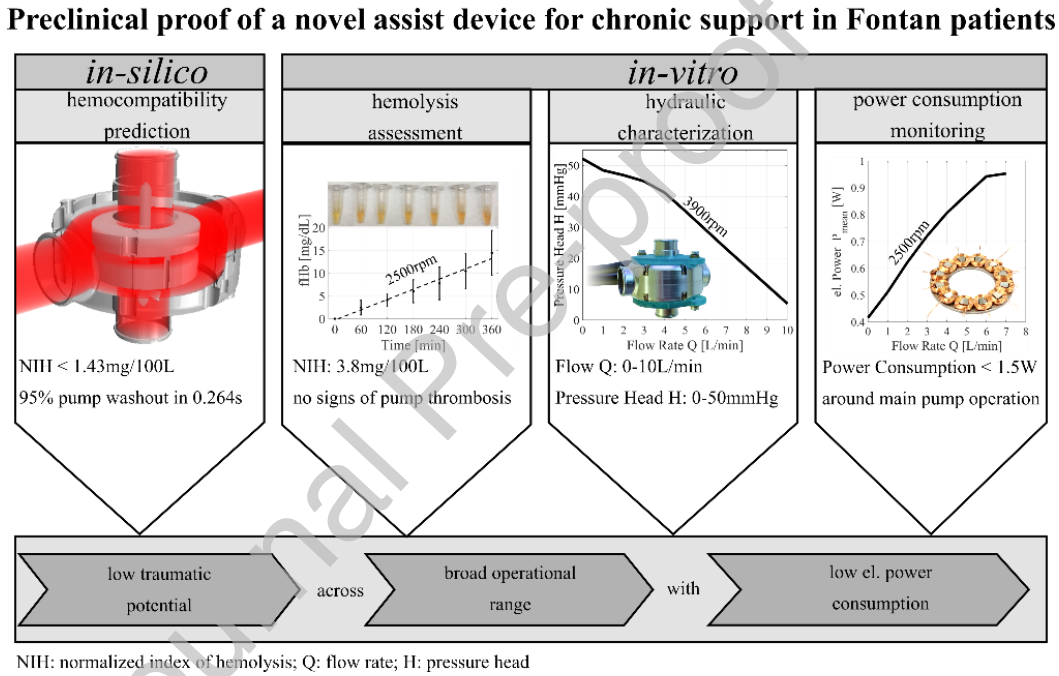

Figure 8. Preclinical evaluation (in-silico, in-vitro) of the CPAD indicated the potential for low traumatic support at low power consumption and across a broad range of hemodynamic conditions (Q=0-10L/min, H=0-50mmHg). CPAD: cavopulmonary assist device; Q: flow rate; H: pressure head.

In recent years, the scientific community has witnessed subtle progress in the field of long-term mechanical cavopulmonary support. Rodefeld et al.[10] were the first to describe the potential for cavopulmonary support using a double-inlet, double-outlet rotary blood pump (RBP) - a seminal work that was continued in the past decade.[20] Their actual device design aims at modest pressure step-ups around 6mmHg arguing such low head pressure levels to

potentially suffice for chronic restoration of biventricular equivalency under physiologic conditions. To date, it remains controversially discussed whether such low cavopulmonary pressure rise is reliably sufficient, particularly in a heterogenous Fontan population with distinct pursuits of physical activity and potentially accompanying secondary disorders (e.g. elevated PVR or systemic ventricular insufficiency).

We believe that chronic cavopulmonary support should be accessible to a heterogenous population including pediatric and adult patients at distinct health states and individual pursuits of physical activity. Consequently, the aspiration of this study was to develop a CPAD operating at wide ranges of pressure step-up's (H=0-50mmHg) and flow rates (Q=0-10L/min) to permit sufficient freedom for physiologically controlled, comprehensive destination therapy in an inclusive Fontan population. To enhance hemodynamic condition and avoid impaired venous return during physical activity, a physiologic control algorithm for automated speed modulation is anticipated as either sensor-based[32] or sensor-less[33] strategy.

An assistive device capable to work in a similarly broad operational range was recently introduced for long-term mechanical support of Fontan patients.[21] Accomplishing the first successful completion of a chronic *in-vivo* trial with a right heart substitute, feasibility for chronic CPAD implantation was underpinned. Yet, this CPAD is currently constrained by considerably larger dimensions and markedly elevated electric power consumption as compared to the herein presented device.

The demand for low traumatic operation covering all clinically relevant hemodynamic conditions imposes intricate challenges: RBPs are designed for a distinct operating condition, accompanied by adverse flow conditions during off-design operation.[28]

Nevertheless, *in-silico* simulations disclosed suitability of the CPAD for efficient support across an inclusive patient population of distinct health states (η_{hyd}>30% at Q=3-8L/min). With 1.77% and 4.15% of the blood volume being exposed to velocities below 0.1m/s and 0.2m/s, respectively, during design point operation, the CPAD can be attested similar blood stagnation potential as compared to the frequently implanted HeartWare Ventricular Assist Device (HVAD, Medtronic, Minneapolis, USA)[28] and the HM3.[29] Additionally, the CPAD proved effective pump washout with periods for 90% and 95% replacement of old blood remaining below values reported for the HVAD[28] and the HM3,[29] respectively.

Further, volume shear exposures above 9, 50 and 150Pa indicative for potential von Willebrand factor cleavage, platelet activation and hemolysis within the CPAD, respectively, remained below magnitudes computed for conventional left ventricular assist devices (LVADs).[28] Even during off-design operation the computed NIH in the CPAD remained more than 10 times below values numerically predicted for design point operation of conventional LVADs.[28]

Noteworthy, the distinct operation across different pressure heads prohibits direct comparability among a CPAD and an LVAD. However, since comparative data of numerical flow analysis in CPADs is missing, such references are deemed valuable to draw conclusions about the eligibility of applying an RBP in cavopulmonary position. The close agreement among CFD and *in-vitro* data (H: RMSE<0.92mmHg, M: RMSE<0.04mNm, Supplementary Section 5) supports validity of the numerical results.

In-silico hemocompatibility findings were complemented by *in-vitro* hemolysis experiments. Experimentally determined values of NIH were more than an order of magnitude smaller than values presented by Giridharan et al.[34] but exceeded levels reported by Cysyk et al. by nearly factor 4.[21] Yet, direct comparability with the latter studies is hampered given the

consideration of different operating conditions. Nevertheless, combined with the twofold reduction in NIH as compared to the HVAD in design point settings,[28] the current prototype without optimized surface finishing points towards a promising hydraulic design.

Aside above hemocompatibility considerations, the CPAD additionally needs to comply with key safety requirements. On the one hand, the risk of pulmonary arteriovenous malformations[24] is to be minimized. For this purpose, the CPAD promotes equally mixed hepatic flow supply to both LPA and RPA even in the event of imbalanced inflow conditions (IR= 2:1, 3:1). On the other hand, the device implantation in TCPC position and thus in series with the cardiovascular system will render the Fontan circulation inherently reliant on the device. Accordingly, device dysfunction with consequent flow obstruction might lead to detrimental hemodynamic compromise. Hence, low pressure loss across a stalled pump is of outmost importance to prevent ultimate failure of the systemic venous circulation in case of device dysfunction.

To this end Rodefeld et al.[20] realized a CPAD with a motor stator in the hub and rotor magnets in the impeller, permitting a housing devoid of any geometrically constraining motor stators. Consequently, this enabled wide flow passage between the impeller and housing with marginal flow obstruction (2.8mmHg at 3.9 L/min) in case of device failure. However, such design approaches may be constrained by inefficient operation. Consequently, diversified support including increased pressure step-ups may require high impeller speeds accompanied by raised electric power consumption.

Thus, we realized a CPAD that accounts for a trade-off between efficient, low-traumatic broad-range operation in functional state and low obstructive behavior in the event of pump malfunction (flow resistance: 0.63-3.15mmHg/(L/min) (Wood Units)). Yet, it remains to be

addressed, whether such flow resistance is acceptably tolerated by the patient in case of device dysfunction.

To mitigate the risk of flow obstruction due to device dysfunction, we focused on a failsafe motor conception by redundant dual motor configuration. In addition, the experience with the HM3 may indicate device malfunction (1.6% at 2 years)[35] and pump thrombosis (<0.01 events per patient-year)[36] to be considered a rare event in RBPs with similar design characteristics. Thus, features which may contribute to this excellent failure rate and outcomes of the HM3 (large gap design of 500µm may prevent occlusive pump thrombosis) were integrated in the proposed CPAD. This contrasts with other devices presented for the same application that incorporate tiny clearance gaps.[20,21]

Given the large gap dimensions within the CPAD, efforts were taken to optimize the size and efficiency of the electric motors. Around its clinically most relevant operating points, the electric power expenditure of the CPAD (<1.5W) was substantially below values reported for contemporary MCS devices and the long-term cavopulmonary support systems introduced above.[20,21] Further, the monotonic relationship between power consumption and pump flow with discernible dependence on imbalanced IR's revealed the potential for robust and reliable pump flow estimation based on intrinsic pump parameters even in light of varying IR's.[37] Omitting the need for additional sensors, such neat approaches could create new avenues for informed monitoring of the cardiovascular system's state in response to device support.

The integration of TET technologies requires the CPAD to accommodate an internal TET component whose implantable battery size proportionally scales with the pump's power demand. Thus, considering a usable volumetric energy density of 0.125 Wh/mL,[38] the herein presented low electric power consumption may permit the battery size to be reduced by approximately 70% compared to equivalent application in current LVADs which run at

higher power expenditures. Hence, the design of a fully implantable system with TET technologies seems promising and may substantially facilitate long-term support of Fontan patients at high patient mobility with eliminated risk for driveline associated adverse events.

Limitations

Except for the *in-silico* analysis of the IVC/SVC mixing behavior during IR's of 2:1 and 3:1, respectively, the numerical simulations presented herein are limited to the representative consideration of a typical IR of 2:1.

Further, the reliable numerical estimation of NIH across the operational range is hampered by substantial discrepancies in magnitudes among *in-silico* and *in-vitro* data. This constitutes the well-known limitation of current *in-silico* hemolysis predictions being constrained to comparative evaluations, while failing to replicate absolute measures. Further, direct comparison of NIH computations with *in-vitro* measurements is hindered given the assumption of smooth surfaces in the simulation setup as opposed to the surfaces in the current prototype that lacks optimal surface finish.

Device implantability was yet solely investigated in a virtual fitting study of a 11-year-old patient.[22] Feasibility to implant the herein presented device in a heterogenous Fontan population remains to be confirmed in a larger virtual fitting study that also accounts for younger patients with strongly limited anatomical space.

Conclusion

Given the inclusive operational range, the promising hemocompatibility properties and the low electric power consumption the proposed cavopulmonary assist may offer a promising option for the long-term therapy of Fontan patients. These findings underpin the rational for

further development by means of acute and chronic *in-vivo* investigations to confirm hemodynamic benefit in chronic disease associated with the Fontan circulation.

Acknowledgements

The work was supported by the North-German Supercomputing Alliance (HLRN). The computational results presented have been achieved in part using the Vienna Scientific Cluster (VSC). This study was supported by the GIGAX Foundation.

References

1. O'Leary PW. Prevalence, clinical presentation and natural history of patients with single ventricle. *Prog Pediatr Cardiol*. 2002;16(1):31-38. doi:10.1016/S1058-9813(02)00042-5

2. Gewillig M. The Fontan circulation. *Heart*. 2005;91(6):839-846. doi:10.1136/hrt.2004.051789

3. Atz AM, Zak V, Mahony L, et al. Longitudinal Outcomes of Patients With Single Ventricle After the Fontan Procedure. *J Am Coll Cardiol*. 2017;69(22):2735-2744. doi:10.1016/j.jacc.2017.03.582

4. De Leval MR. The Fontan circulation: What have we learned? What to expect? *Pediatr Cardiol*. 1998;19(4):316-320. doi:10.1007/s002469900315

5. Rychik J. The Relentless Effects of the Fontan Paradox. *Semin Thorac Cardiovasc Surg Pediatr Card Surg Annu*. 2016;19(1):37-43. doi:10.1053/j.pcsu.2015.11.006

6. Goldberg DJ, Shaddy RE, Ravishankar C, Rychik J. The failing Fontan: Etiology, diagnosis and management. *Expert Rev Cardiovasc Ther*. 2011;9(6):785-793.

doi:10.1586/erc.11.75

7. Rychik J, Atz AM, Celermajer DS, et al. Evaluation and Management of the Child and Adult with Fontan Circulation: A Scientific Statement from the American Heart Association. *Circulation*. 2019;140(6):E234-E284. doi:10.1161/CIR.0000000000000696

8. Karamlou T, Hirsch J, Welke K, et al. A United Network for Organ Sharing analysis of heart transplantation in adults with congenital heart disease: Outcomes and factors associated with mortality and retransplantation. *J Thorac Cardiovasc Surg*. 2010;140(1):161-168. doi:10.1016/j.jtcvs.2010.03.036

9. Schilling C, Dalziel K, Nunn R, et al. The Fontan epidemic: Population projections from the Australia and New Zealand Fontan Registry. *Int J Cardiol*. Published online 2016. doi:10.1016/j.ijcard.2016.05.035

10. Rodefeld MD, Coats B, Fisher T, et al. Cavopulmonary assist for the univentricular Fontan circulation: Von Kármán viscous impeller pump. *J Thorac Cardiovasc Surg*. 2010;140(3):529-536. doi:10.1016/j.jtcvs.2010.04.037

11. Haggerty CM, Fynn-Thompson F, McElhinney DB, et al. Experimental and numeric investigation of Impella pumps as cavopulmonary assistance for a failing Fontan. *J Thorac Cardiovasc Surg*. 2012;144(3):563-569. doi:10.1016/j.jtcvs.2011.12.063

12. Prêtre R, Häussler A, Bettex D, Genoni M. Right-Sided Univentricular Cardiac Assistance in a Failing Fontan Circulation. *Ann Thorac Surg*. 2008;86(3):1018-1020. doi:10.1016/j.athoracsur.2008.03.003

13. Valeske K, Yerebakan C, Mueller M, Akintuerk H. Urgent implantation of the Berlin Heart Excor biventricular assist device as a total artificial heart in a patient with single

ventricle circulation. *J Thorac Cardiovasc Surg*. 2014;147(5):1712-1714. doi:10.1016/j.jtcvs.2014.01.012

14. Halaweish I, Ohye RG, Si MS. Berlin heart ventricular assist device as a long-term bridge to transplantation in a Fontan patient with failing single ventricle. *Pediatr Transplant*. 2015;19(8):E193-E195. doi:10.1111/petr.12607

15. Weinstein S, Bello R, Pizarro C, et al. The use of the Berlin Heart EXCOR in patients with functional single ventricle. *J Thorac Cardiovasc Surg*. 2014;147(2):697-704; discussion 704-5. doi:10.1016/j.jtcvs.2013.10.030

16. Arnaoutakis GJ, Blitzer D, Fuller S, et al. Mechanical Circulatory Support as Bridge to Transplantation for the Failing Single Ventricle. *Ann Thorac Surg*. 2017;103(1):193-197. doi:10.1016/j.athoracsur.2016.05.015

17. Horne D, Conway J, Rebeyka IM, Buchholz H. Mechanical Circulatory Support in Univentricular Hearts: Current Management. *Semin Thorac Cardiovasc Surg Pediatr Card Surg Annu*. 2015;18(1):17-24. doi:10.1053/j.pcsu.2015.02.002

18. Adachi I, Burki S, Fraser C. Current status of pediatric ventricular assist device support. *Semin Thorac Cardiovasc Surg Pediatr Card Surg Annu*. 2017;20:2-8. Accessed March 6, 2020. https://www.sciencedirect.com/science/article/pii/S1092912616300114

19. Woods RK, Ghanayem NS, Mitchell ME, Kindel S, Niebler RA. Mechanical Circulatory Support of the Fontan Patient. *Semin Thorac Cardiovasc Surg Pediatr Card Surg Annu*. 2017;20:20-27. doi:10.1053/j.pcsu.2016.09.009

20. Rodefeld MD, Marsden A, Figliola R, Jonas T, Neary M, Giridharan GA. Cavopulmonary assist: Long-term reversal of the Fontan paradox. In: *Journal of*

Thoracic and Cardiovascular Surgery. Vol 158. Mosby Inc.; 2019:1627-1636. doi:10.1016/j.jtcvs.2019.06.112

21. Cysyk J, Clark JB, Newswanger R, et al. Chronic In Vivo Test of a Right Heart Replacement Blood Pump for Failed Fontan Circulation. *ASAIO J*. 2019;65(6):593-600. doi:10.1097/MAT.0000000000000888

22. Granegger M, Thamsen B, Hubmann E, et al. A Long-term Mechanical Cavopulmonary Support Device for Patients with Fontan Circulation. *Med Eng Phys*. 2019;70:9-18. doi:10.1016/j.medengphy.2019.06.017

23. Zernetsch H, Repanas A, Rittinghaus T, Mueller M, Alfred I, Glasmacher B. Electrospinning and Mechanical Properties of Polymeric Fibers Using a Novel Gap-spinning Collector. *Fibers Polym*. 2016;17(7):1025-1032. doi:10.1007/s12221-016-6256-7

24. Kavarana MN, Jones JA, Stroud RE, Bradley SM, Ikonomidis JS, Mukherjee R. Pulmonary arteriovenous malformations after the superior cavopulmonary shunt: Mechanisms and clinical implications. *Expert Rev Cardiovasc Ther*. 2014;12(6):703-713. doi:10.1586/14779072.2014.912132

25. Klimes K, Abdul-Khaliq H, Ovroutski S, et al. Pulmonary and caval blood flow patterns in patients with intracardiac and extracardiac Fontan: A magnetic resonance study. *Clin Res Cardiol*. 2007;96(3):160-167. doi:10.1007/s00392-007-0470-z

26. Hubmann EJ, Bortis D, Flankl M, Kolar JW, Granegger M, Hubler M. Optimization and Calorimetric Analysis of Axial Flux Permanent Magnet Motor for Implantable Blood Pump Assisting the Fontan Circulation. In: *2019 22nd International Conference on Electrical Machines and Systems, ICEMS 2019*. ; 2019. doi:10.1109/ICEMS.2019.8921580

27. Garon A, Farinas M-I. Fast Three-dimensional Numerical Hemolysis Approximation. *Artif Organs*. 2004;28(11):1016-1025. doi:10.1111/j.1525-1594.2004.00026.x

28. Granegger M, Thamsen B, Schlöglhofer T, et al. Blood trauma potential of the HeartWare Ventricular Assist Device in pediatric patients. *J Thorac Cardiovasc Surg*. 2020;159(4):1519-1527. doi:10.1016/j.jtcvs.2019.06.084

29. Wiegmann L, Thamsen B, de Zélicourt D, et al. Fluid Dynamics in the HeartMate 3: Influence of the Artificial Pulse Feature and Residual Cardiac Pulsation. *Artif Organs*. 2019;43(4):363-376. doi:10.1111/aor.13346

30. Strauch C, Escher A, Granegger M, Thamsen PU. Experimental hydraulic and mechanical characterisation of a double-flow implantable blood pump. In: Proceedings of the ASME 2020 Fluids Engineering Division Summer Meeting FEDSM2020.

31. Sundareswaran KS, Reichenbach SH, Masterson KB, Butler KC, Farrar DJ. Low Bearing Wear in Explanted HeartMate II Left Ventricular Assist Devices After Chronic Clinical Support. *ASAIO J*. 2013;59(1):41-45. doi:10.1097/MAT.0b013e3182768cfb

32. Granegger M, Schweiger M, Schmid Daners M, Meboldt M, Hübler M. Cavopulmonary mechanical circulatory support in Fontan patients and the need for physiologic control: A computational study with a closed-loop exercise model. *Int J Artif Organs*. 2018;41(5):261-268. doi:10.1177/0391398818762359

33. Wang Y, Peng J, Rodefeld MD, Luan Y, Giridharan GA. A sensorless physiologic control strategy for continuous flow cavopulmonary circulatory support devices. *Biomed Signal Process Control*. 2020;62:102130. doi:10.1016/j.bspc.2020.102130

34. Giridharan GA, Koenig SC, Kennington J, et al. Performance evaluation of a pediatric

viscous impeller pump for Fontan cavopulmonary assist. *J Thorac Cardiovasc Surg*. 2013;145(1):249-257. doi:10.1016/j.jtcvs.2012.01.082

35. Mehra MR, Goldstein DJ, Uriel N, et al. Two-Year Outcomes with a Magnetically Levitated Cardiac Pump in Heart Failure. *N Engl J Med*. 2018;378(15):1386-1395. doi:10.1056/NEJMoa1800866

36. Goldstein D, Naka Y, Horstmanshof D, et al. Association of clinical outcomes with left ventricular assist device use by bridge to transplant or destination therapy intent: the multicenter study of MagLev technology. *JAMA Cardiol*. 2020;5(4):411-419. Accessed April 19, 2021. https://jamanetwork.com/journals/jamacardiology/article-abstract/2758869

37. Granegger M, Moscato F, Casas F, Wieselthaler G, Schima H. Development of a pump flow estimator for rotary blood pumps to enhance monitoring of ventricular function. *Artif Organs*. 2012;36(8):691-699. doi:10.1111/j.1525-1594.2012.01503.x

38. Knecht O, Kolar JW. Performance Evaluation of Series-Compensated IPT Systems for Transcutaneous Energy Transfer. *IEEE Trans Power Electron*. 2018;34(1):438-451. doi:10.1109/TPEL.2018.2822722

Legend Section

Figure 1. Mechanical design of the CPAD for implantation in TCPC position. A. CPAD implanted in TCPC location between IVC, SVC, LPA and RPA in a heart with single ventricle (SV).[22] Blood is entering the flow chamber through its inflow cannulae that are connected to the IVC and SVC, and radially ejected through its outlet cannulae which are anastomosed to the LPA and RPA, respectively. B. CAD explosion view of the CPADthat is composed of a four-bladed impeller which is suspended within the circular flow chamber using mechanical ball-cup bearings. Via driveline, the impeller is actuated by the electromagnetic force that is generated by the coupling between motor rotor and motor stator. The stators are protected from corrosion by means of 3D-printed stator cap prototypes. C. Functional prototype of the CPAD (top) including the setting with both its in- and outlets connected to the custom-made electrospun conical grafts (bottom). Distal ends of the cannula in- and outlets are spaced by 34mm and 40mm, respectively. The total volume of the CPAD amounts to a magnitude of 17.8cm^3. D. Illumination of the small-sized conception of the current functional prototype. CPAD: cavopulmonary assist device; TCPC: total cavopulmonary connection; IVC: inferior vena cava; SVC: superior vena cava; LPA: left pulmonary artery: RPA: right pulmonary artery; SV: single ventricle; CAD: computer aided design.

Figure 2. In-silico and in-vitro hydraulic characterization of the CPAD. A. In-silico setup for hydraulic characterization and hemolysis prediction numerically showing the blood circulation through the CPAD. B. CPAD connected to the TCPC-imitating configuration of the in-vitro testbench. The functional prototype of the CPAD was integrated into the testbench via four 3/8'' silicon tubings of equal length (L=65mm) that were furthermore connected to the four pressure sensors (p_{IVC}, p_{SVC}, p_{LPA}, p_{RPA}). White circles denote the pressure sensors, while the red arrows indicate blood flow direction. CPAD: cavopulmonary assist device; TCPC: total cavopulmonary connection; p_{SVC}: pressure superior vena cava; p_{IVC}: pressure inferior vena cava; p_{LPA}: pressure left pulmonary artery; p_{RPA}: pressure right pulmonary artery.

Figure 3. In-silico hydraulic performance and blood trauma prediction. A. Numerically computed hydraulic efficiency of the CPAD with three exemplary pressure-flow curves (n=1800, 2500, 3200rpm, IR=2:1) indicating a comprehensive operational range of high hydraulic efficiency (η_{hyd}>30%) performance. B. Numerically predicted NIH for the CPAD operated at rotational speeds of 1800, 2500 and 3200rpm with an IR of 2:1 indicating an increase towards low-flow operation, however with low-level values (NIH<1.43mg/100L) across a broad clinically relevant range. C. Computed blood volume portions exposed to shear stresses above 9, 50 and 150Pa across the pump's operational range (IR=2:1), expressed as percentage of the pump's priming volume. Volumes exposed to the respective shear stress levels tend to increase with increasing flow rate. CPAD: cavopulmonary assist device; n: rotational speed; IR: inflow ratio; NIH: normalized index of hemolysis.

Figure 4. Numerical prediction of old blood washout and IVC/SVC blood mixing behavior. A. In the process of the virtual washout experiment the CPAD is run with design point settings (n=2500rpm, Q=4L/min, H=12.55mmHg, IR=2:1), while old blood (visualized in red, t_1) is continuously replaced with the newly entering blood represented in blue. After 3 revolutions (t_2=0.072s) the new blood is increasingly mixing with the old blood consequently displacing the old blood towards the LPA and RPA outlets. After 8 revolutions (t_3=0.192s), 87.83% of the old blood is replaced with new blood. B. During design point operation (n=2500rpm, Q=4L/min, H=12.55mmHg), however, with highly imbalanced IR of 3:1 blood that is entering through the IVC (denoted as dark blue) is homogeneously mixed with the inflowing blood of the SVC, equalizing outflow distribution of IVC-blood to both LPA and RPA outlet. IVC: inferior vena cava; SVC: superior vena cava; LPA: left pulmonary artery; RPA: right pulmonary artery; CPAD: cavopulmonary assist device; n: rotational speed; Q: flow rate; H: pressure head; IR: inflow ratio.

Figure 5. Pressure-flow relationship indicating the hydraulic performance of the CPAD. Pressure heads were recorded in-vitro for the operation at rotational speeds between 1500 and 3900rpm with flow rates ranging from 0 to 8L/min. At each flow rate, in-vitro data is presented as mean and standard deviation (error bars) among pressure heads recorded for balanced (1:1) and imbalanced (2:1, 3:1) IR's. Black makers represent the numerically computed pressure-flow relationship (CFD) at selected rotational speeds (1800, 2500, 3200rpm) for flow rates among 0 to 10L/min and an IR of 2:1. Pressure-loss across the CPAD in case of stalled pump condition (n=0rpm) is illustrated as light green line. CPAD: cavopulmonary assist device; IR: inflow ratio; CFD: computational fluid dynamics; n: rotational speed.

Figure 6. In-vitro hemolysis assessment. Increasing concentration of plasma free hemoglobin (fHb) during in-vitro hemolysis experiments (N=3) of 6h design point operation each (2500rpm, 4L/min, IR=2:1). At each sampling time point (Δt=60min), in-vitro data is presented as median and standard deviation (error bars) of the photometrically determined concentration in plasma free hemoglobin across the three distinct experiments. The top row shows the Eppendorf tubes with isolated blood plasma at each sampling time, illustrating the rise of plasma free hemoglobin by increasing red-scale over time. fHb: free Hemoglobin; N: number of experiments; IR: inflow ratio.

Figure 7. Electric power consumption of the CPAD. The power consumption was monitored across a clinically relevant range with flow rates between 0 to 8L/min and at rotational speeds of 1500 to 3900rpm, showing monotonic behavior across the entire operational range. Measured data is presented at each flow rate as mean and standard deviation (error bars) among balanced (1:1) and imbalanced (2:1, 3:1) IR's with the solid line representing the interpolation between measurement points. CPAD: cavopulmonary assist device; IR: inflow ratio.

Figure 8. Preclinical evaluation (in-silico, in-vitro) of the CPAD indicated the potential for low traumatic support at low power consumption and across a broad range of hemodynamic conditions (Q=0-10L/min, H=0-50mmHg). CPAD: cavopulmonary assist device; Q: flow rate; H: pressure head.

Video 1. This video provides an illustration of the clinical challenges that are accompanying patients with established Fontan circulation. It indicates the unmet medical need of an appropriate long-term treatment option for the heterogeneous Fontan population and proposes a novel cavopulmonary assist device as a potential solution for chronic restoration of biventricular equivalency. Further, this video provides insight into key aspects of the device design, preclinical evaluation and corresponding clinical implications.